

Article

Superior Performance Nanocomposites from Uniformly Dispersed Octadecylamine Functionalized Multi-Walled Carbon Nanotubes

Ye Chen ¹, Jing Tao ¹, Alaa Ezzeddine ¹, Remi Mahfouz ², Abdullah Al-Shahrani ², Gasan Alabedi ² and Niveen M. Khashab ^{1,*}

¹ Smart Hybrid Materials (SHMs), Advanced Membranes and Porous Materials Center, King Abdullah University of Science and Technology (KAUST), Thuwal 23955-6900, Saudi Arabia; E-Mails: tedchan123@163.com (Y.C.); rechall1101@gmail.com (J.T.); alaa.ezzeddine@kaust.edu.sa (A.E.)

² Oil & Gas Network Integrity Research Team, Research and Development Center, Saudi Aramco, Dhahran 31311, Saudi Arabia; E-Mails: remi.mahfouz@aramco.com (R.M.); abdullah.shahrani.13@aramco.com (A.A.-S.); gasan.alabedi@aramco.com (G.A.)

* Author to whom correspondence should be addressed; E-Mail: niveen.khashab@kaust.edu.sa; Tel.: +966-2802-1172; Fax: +966-2808-2410.

Academic Editor: Vijay Kumar Thakur

Received: 21 October 2015 / Accepted: 1 December 2015 / Published: 8 December 2015

Abstract: Polyetherimide (PEI) is a widely applied as engineering plastic in the electronics, aerospace, and automotive industries but the disadvantages of extremely low conductivity, atmospheric moisture absorption, and poor fluidity at high temperature limits its application. Herein, commercial multi-walled carbon nanotubes (MWCNTs) were modified with a long alkyl chain molecule, octadecylamine (ODA), to produce a uniform dispersion in commercial PEI matrices. Both covalent and noncovalent modification of MWCNTs with ODA, were prepared and compared. Modified MWCNTs were incorporated in PEI matrices to fabricate nanocomposite membranes by a simple casting method. Investigating mechanical properties, thermal stability, and conductivity of the polyetherimide (PEI)/MWCNT composites showed a unique combination of properties, such as high electrical conductivity, high mechanical properties, and high thermal stability at a low content of 1.0 wt % loading of ODA modified MWCNTs. Moreover, electrical resistivity decreased around 10 orders of magnitude with only 0.5 wt % of modified MWCNTs.

Keywords: polyetherimide; multi-walled carbon nanotubes; octadecylamine; mechanical properties; electrical properties

1. Introduction

Polyetherimide (PEI) is widely used as an engineering plastic in the electronics, aerospace, and automotive industries due to its high thermal stability, good mechanical properties, and radiation resistance. Some drawbacks include extremely low conductivity, atmospheric moisture absorption, and poor fluidity at high temperature, which greatly limits its application. Many efforts to improve its properties by adding carbon nanotubes (CNT) [1–3] or graphitic nanoplatelets (GNP) [4] into the matrix, or compositing with other special structure materials such as liquid crystalline polymer (LCP) [5,6] or carbon nanofibers (CNF) have been reported [7,8]. Carbon nanotubes have drawn large attention as “materials of the 21st century” due to their impressive physical and chemical properties since their serendipitous discovery in 1991 [9]. Their excellent electronic, mechanical, and thermal properties make them a great candidate filler for the reinforcement of commercial plastics [10–17].

Compared to single-walled carbon nanotubes (SWCNTs), multi-walled carbon nanotubes (MWCNTs) are cheaper, and are used more widely in application of polymer/CNT composites. The high performance PEI/MWCNT composite can be considered as a multi-functional material in the next generation of aircraft or other applications where saving weight and multi-functionality are required. The dispersion of CNT in common solvents is usually poor because of the strong tendency to aggregate due to the large surface/volume ratio and strong van der Waals forces [18]. Thus, the homogeneous dispersion of CNT in the plastic matrix is one of the most critical factors for successful composite applications [17].

A tremendous effort has been invested in developing stable and well-dispersed CNTs in organic solvents. Two major methods have been reported: covalent [19–24] and noncovalent [25–32] functionalization. Compared to the covalent functionalization, the main advantage of the noncovalent functionalization is that the chemical groups can be introduced to the CNT surface without disrupting the intrinsic structure and electronic network [33]. The advantage of covalent functionalization is that functional groups can be covalently linked to the surface of CNT and the linkage is mechanically stable and permanent at the cost of breaking of the sp^2 conformation of the carbon atom. Therefore, CNT modified with the covalent method are usually more stable and more easily controlled. There have been several covalent methods reported to achieve high performance PEI/MWCNT composite. Cheng *et al.* [23] used MWCNT modified with grafting PEI to get MWCNT/PEI composites, the MWCNTs were found to disperse well in polymer matrix. The tensile strength and modulus of PEI composite grafted with MWCNT increased dramatically with the MWCNTs' concentration. Other methods including ultrasound and melting blend were involved in improving the dispersion of MWCNT in polymer matrix [34,35]. Isayev *et al.* [35] developed a solvent free, with no surface modification needed and new ultrasound-assisted twin screw extrusion method for manufacturing PEI/MWNT nanocomposites. The mechanical properties data shows that MWCNT loading and ultrasound have a positive effect on the tensile strength and Young's modulus of the nanocomposites.

Long-chain molecules, octadecylamine (ODA), were used first to help in dissolving single-walled carbon nanotubes (SWCNTs) in solvent [36]. Due to the strong interaction of ODA with CNT via formation of amides and the breakdown of CNT bundles, SWCNTs grafted with ODA were found well dispersed in organic solvent [37]. Not only SWCNTs with covalent functionalization, but also with non-covalent functionalization could be dispersed well in solvents, which provided us with a straightforward method to make homogeneous nanotube-based copolymers and polymer composites [38]. Xu *et al.* [39] found that ODA chains grafted with multi-walled carbon nanotubes (MWCNTs) were partially crystallized, and they thought that ODA preferred to react at the tube-ends and the defects on the sidewall of MWCNTs. Although ODA can be used to improve the solubility or dispersability of CNT, the application of CNT modified with ODA in plastic nanocomposites is rarely reported. In a very recent report, Salavagione *et al.* [40] used MWCNT grafted with a long chain molecule 1-octadecylalcohol to improve the solubility of MWCNT in poly(vinyl chloride) (PVC) matrix. No indications were presented whether this effect can be used in other commercial polymeric systems. In our study, octadecylamine (ODA) was utilized to functionalize commercial MWCNT–COOH by both covalent and noncovalent methods. The mechanical properties, thermal stability, and conductivity of the polyetherimide (PEI)/MWCNT composites were investigated and compared based on these two kinds of functionalized MWCNTs.

2. Results and Discussion

2.1. Dispersion Behavior of Functionalized Multi-Walled Carbon Nanotube (MWCNT) in Dichloromethane (DCM)

The dispersion behaviors of the *c*-MWCNT–ODA, *n*-MWCNT–ODA and the pristine MWCNT–COOH samples are studied in DCM (the concentration of nanoparticles in DCM was 0.2 wt %). Based on the visual characteristic of the dispersion, sedimentation can clearly be observed for the pristine MWCNT–COOH because of the strong van der Waals interaction between the sidewalls of the MWCNT [3], while for the *c*-MWCNT–ODA and the *n*-MWCNT–ODA, no precipitate of black agglomeration was observed. The good dispersion of functionalized MWCNTs in DCM supports the preparation of homogenous mixture of MWCNTs and PEI.

2.2. The Confirmation of Octadecylamine (ODA) Modified MWCNTs

Fourier transform infrared spectroscopy (FTIR), X-ray powder diffraction (XRD), and thermogravimetric analysis (TGA) were used to confirm the functionalization of MWCNTs with ODA. As shown in Figure 1a of FTIR result, the peak at 1720 cm^{-1} of MWCNT–COOH sample is due to C=O stretch mode in carboxylic acid, indicating the COOH group in our pristine MWCNT–COOH sample, and the peak at 1625 cm^{-1} is due to the backbone vibration of carbon nanotubes. The peaks at 2918 cm^{-1} and 2850 cm^{-1} in sample of *c*-MWCNT–ODA belong to the C–H stretching vibration of the alkyl chain ($\nu(\text{CH}_2, \text{CH}_3)$), and the same peaks appear in *n*-MWCNT–ODA and pristine ODA samples. In the sample of *c*-MWCNT–ODA, the peak at 1720 cm^{-1} almost disappears, and the peak at 1635 cm^{-1} is probably due to the stretching vibration of the amide carbonyl group ($\nu(\text{C}=\text{O})$), indicating the formation of the carboxylate group, which is a strong evidence for the successful covalent functionalization of MWCNT

with ODA [39]. The small shoulder at 1557 cm^{-1} of *c*-MWCNT-ODA is probably due to the N-H bend of the amide, while the same peak appears at 1570 cm^{-1} and 1565 cm^{-1} in pristine ODA and *n*-MWCNT-ODA, respectively[37]. The peak at 1085 cm^{-1} in *c*-MWCNT-ODA and 1082 cm^{-1} in *n*-MWCNT-ODA is probably due to the shift of C-N stretch at 1022 cm^{-1} in parent amine ODA. The peak at 1466 cm^{-1} of ODA belongs to the C-H bend, and it moves to 1460 cm^{-1} in *c*-MWCNT-ODA and *n*-MWCNT-ODA sample. The spectral shifts observed in Figure 1 might result from the functionalized ODA with MWCNT.

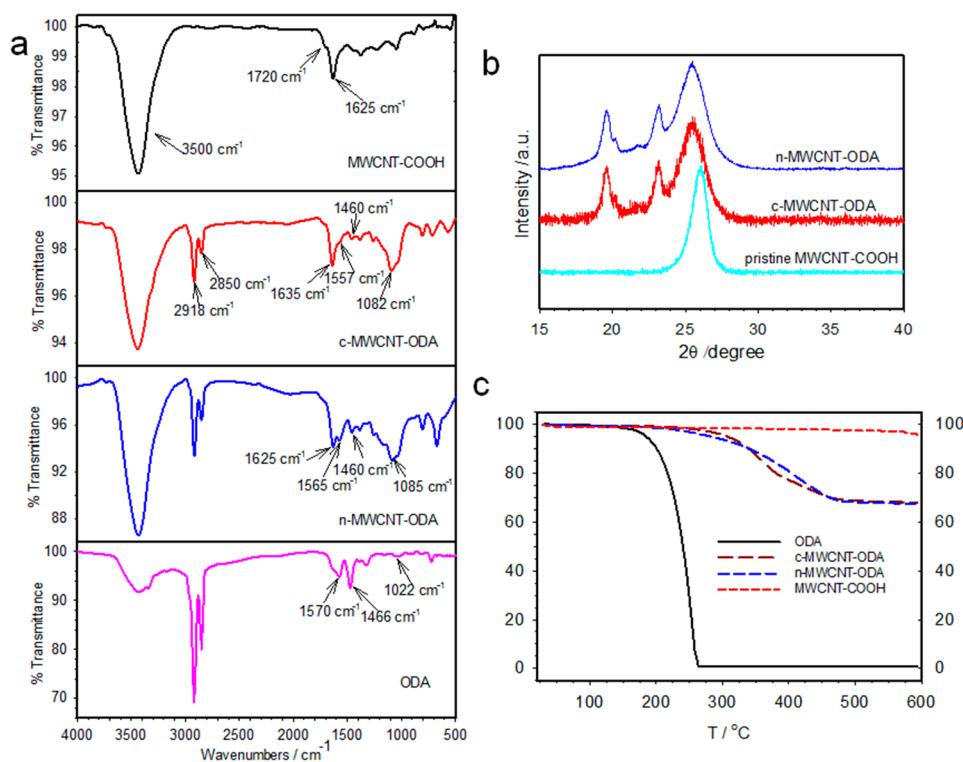


Figure 1. IR spectrum (a); XRD (b); and TGA weight loss curves (c) of pristine MWCNT-COOH and ODA-modified MWCNTs.

As shown in Figure 1b of XRD results, in the 2θ range of $10\text{--}40^\circ$, there is only one diffraction peak around at $2\theta = 25.8^\circ$ in pristine MWCNT-COOH, a typical reflection peak (0 0 2) in MWCNT, and the d-spacing is about 3.4 \AA . While there are three obvious diffraction peaks of modified MWCNT appearing at $2\theta = 25.4, 23.2$ and 19.6° . In Xu's research [39], they found that the XRD diffraction peak was strongly influenced by adding ODA to MWCNT with different reaction time. In our experiment, the change was also observed. By modifying with ODA, the main diffraction of MWCNT became broader and a slight shift was observed ($2\theta = 25.4^\circ$). The strong interaction of ODA with MWCNT in the *n*-MWCNT-ODA sample and the grafted ODA on MWCNT surface in the *c*-MWCNT-ODA sample may decrease the order of crystallinity in MWCNT or deteriorate the degree of MWCNT crystallinity, which induces the main diffraction peak to become broader and slightly shifting to low angle. This change supports the successful functionalization of ODA to MWCNTs. In addition, two new peaks at around $2\theta = 23.2$ and 19.6° and a small peak near to the peak of $2\theta = 19.6^\circ$ appeared in modified MWCNTs belonged to crystalline ODA, further indicating that ODA was combined to the pristine MWCNTs by both covalent and non-covalent method.

ODA has a low decomposition temperature at near 160 °C (Figure 1c), which means that ODA has poor thermal stability compared with MWCNT–COOH which is still stable at high temperature. As shown in Figure 1c, compared with pristine MWCNT–COOH, the thermal properties of both functionalized MWCNTs are decreased, and *c*-MWCNT–ODA has a better thermal stability than *n*-MWCNT–ODA. The decomposition temperature of *c*-MWCNT–ODA is improved by 20% comparing with *n*-MWCNT–ODA, which indicates that the covalent (chemical) interaction between the MWCNT–COOH and ODA is much stronger than the non-covalent (physical) interaction between them. The onset decomposition of *n*-MWCNT–ODA is around 205 °C, while for *c*-MWCNT–ODA, it is 255 °C. Both of these weights' losses are ascribed to the decomposition of ODA. In the sample of *n*-MWCNT–ODA, ODA has a strong physical interaction with carbon nanotube, and the MWCNTs around ODA molecules will increase the thermal stability of ODA molecules. In the sample of *c*-MWCNT–ODA, ODA was grafted onto MWCNT surface. Compared with *n*-MWCNT–ODA, ODA formed a chemical bond with MWCNT in *c*-MWCNT–ODA, and the protection of MWCNT to ODA molecule was further improved. This can probably explain why the thermal stability of *c*-MWCNT–ODA is higher than *n*-MWCNT–ODA. In addition, a residue weight of 67 wt % is found in both functionalized MWCNTs, which indirectly indicates that the ratio of ODA to MWCNT in functionalized MWCNT is 1:2. And this ratio is good for MWCNT–ODA becoming soluble in organic solvents [37].

The introduction of ODA to MWCNT might cause a change on MWCNT walls' morphology and its nanostructure. To investigate the influence on this, Raman spectrum and TEM images are analyzed. The Raman spectrum of the pristine MWCNT–COOH and the ODA-modified MWCNT with covalent and noncovalent methods are shown in Figure 2. Two strong peaks are observed. One peak around 1580 cm^{-1} is referred as the G band and originates from the tangential vibrations of the carbon atoms. The other one is around 1360 cm^{-1} and is assigned as the D band, which may be caused by the significant defects or disorders in the carbon nanostructures. As shown in Figure 2, there is no Raman shift observed in modified MWCNTs. The relative intensity between the D and the G bands is known to be a good indicator of the quantity of structural defects. In our experiment, it is found that the ratio of D-band and G-band of pristine MWCNT–COOH is 0.588, and that of modified MWCNTs with covalent method and noncovalent are 0.748 and 0.713, respectively, indicating that MWCNT with ODA modification had a slight destructive effects on the surface of CNTs, and the covalent method had a little more damage to CNT surface than noncovalent method.

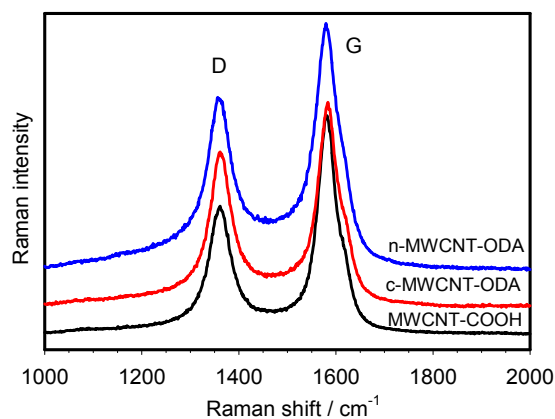


Figure 2. Raman spectra of pristine MWCNT-COOH and modified MWCNTs.

Figure 3 shows the TEM images of pristine MWCNT–COOH and modified MWCNTs. It is found that most of pristine MWCNT–COOH aggregate together to form a large domain. Due to the strong van der Waals forces, the bundle of pristine MWCNT is not easy to destroy. As shown in Figure 3a, most pristine MWCNTs entangle each other. The multi-walls of CNTs are clearly observed under high-resolution mode, and the surface of pristine MWCNT–COOH is almost smooth (Figure 3b). After the modification with ODA molecule, the surface morphology of MWCNT changed. It becomes rough and there are some compounds stacked or wrapped on the surface of MWCNT, which are due to the presence of ODA molecules. The EDS image taken from *c*-MWCNT–ODA clearly identifies the presence of carbon, oxygen, and nitrogen where the signal of nitrogen is assigned to the composition of ODA molecules, not from pristine MWCNT–COOH. The existence of nitrogen in *c*-MWCNT–ODA further confirms the success of ODA grafted onto MWCNT.

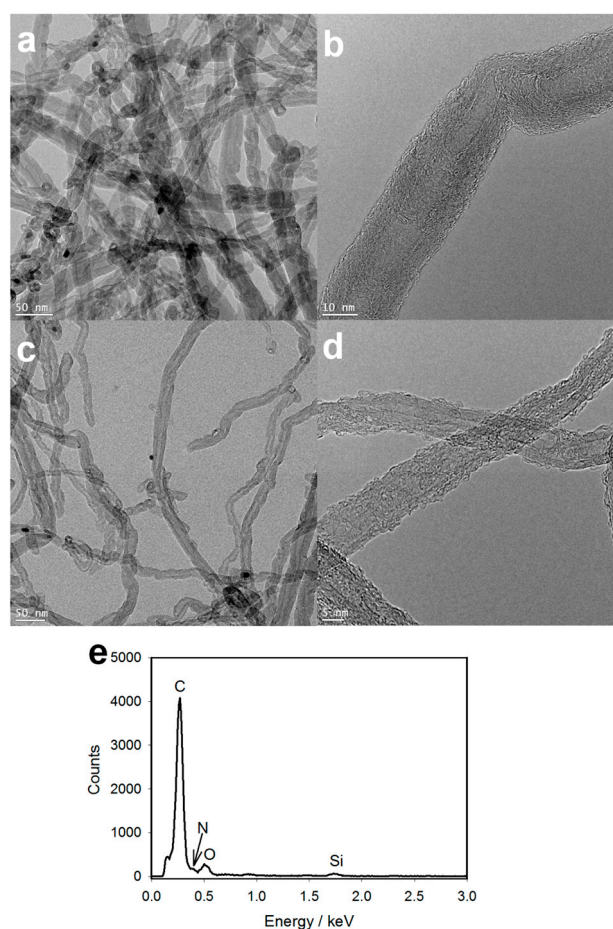


Figure 3. TEM image of pristine MWCNT–COOH (a,b) and *c*-MWCNT–ODA (c,d); and (e) EDS result of *c*-MWCNT–ODA.

2.3. Scanning Electron Microscope (SEM) Study on MWCNT-ODA Dispersed in the Composite Films

SEM characterization shows a remarkable density of fine and homogeneously-dispersed modified MWCNTs at individual level throughout the PEI matrix. The morphology of the fracture surface for the PEI composite film containing 2.0 wt % pristine MWCNT–COOH and 2.0 wt % modified MWCNT are given. As shown in Figure 4, the obvious phase separation is observed in the composite with 2.0 wt %

pristine MWCNT–COOH (Figure 4b), while the morphology (cross section) of neat PEI is found to be homogenous and smooth (Figure 4a). Aggregation of pristine MWCNT–COOH is easily observed in the PEI matrix as shown in Figure 4c. For the cryo-fractured surfaces both of the nanocomposite film with 2.0 wt % *n*-MWCNT–ODA and with 2.0 wt % *c*-MWCNT–ODA, no obvious MWCNT aggregation occurred. As shown in Figure 4d,e, compared with neat PEI surface (Figure 4a), there are many bright dots and lines on the nanocomposite surface of PEI with 2.0 wt % modified MWCNTs, which are the individual MWCNTs dispersed uniformly in PEI matrix, and this is very important for making CNT reinforced polymer nanocomposites with excellent mechanical properties [10]. Moreover, close inspection (Figure 4g,h) indicates that no remarkable physical damages or shortening of MWCNTs are observed, which indicated that ODA modification, both covalent and non-covalent is a mild method that conserves the morphology structure of the nanotubes. In sample of *c*-MWCNT–ODA, the strong adhesion between the *c*-MWCNT–ODA and the matrix means a good wettability between them (Figure 4f,h). Individual *c*-MWCNT–ODA can be easily found shows that the wrapping of modified MWCNT by long alkyl chains of ODA can reduce the van der Waals forces between the MWCNTs efficiently resulting in the well dispersion of MWCNT in the PEI matrix. This is a critical issue for the mechanical properties of the composite because it will contribute to achieving efficient transfer from load to the MWCNT network in the PEI matrix. The good dispersion of MWCNT also help in distributing the stress uniformly and minimize the presence of stress concentrations [10]. As observed from Figure 4g,h, the diameter of functionalized MWCNT in the matrix was much thicker than the pristine one (10–20 nm), and the carbon nanotube was immersed into the polymer matrix (as shown in Figure 4g,h), which means that MWCNT was wrapped by PEI when it dispersed into the polymer matrix. However, some partial re-aggregation of modified MWCNTs were still observed in the polymer matrix, as shown in Figure 4k, which indicated that higher concentration increase the possibility of MWCNT aggregate when stirring the solution. Compared with pristine MWCNTs, the re-aggregation modified MWCNTs are very small in amount.

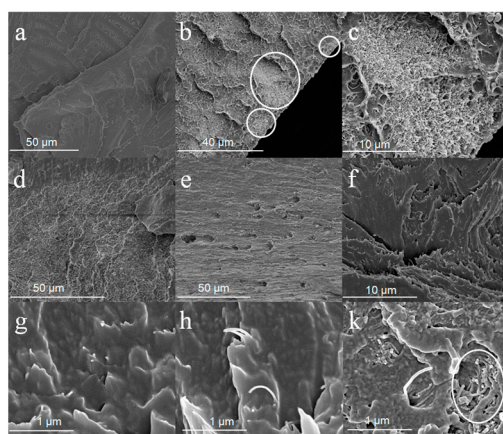


Figure 4. SEM images of neat PEI (a); the nanocomposite film with 2.0 wt % pristine MWCNT–COOH (b,c); the nanocomposite film with 2.0 wt % *n*-MWCNT–ODA (d); the nanocomposite with 2.0 wt % *c*-MWCNT–ODA (e,f), the close observation of *n*-MWCNT–ODA in PEI (g) and *c*-MWCNT–ODA in PEI (h,k). The white circles in (b) are the aggregation domains of pristine MWCNT–COOH, while the white circles in (k) are the partial aggregation of *c*-MWCNT–ODA.

2.4. Thermal Properties of the Composite Films

The thermal behavior of neat PEI membranes and PEI composite membranes with the different MWCNT concentration were studied by TGA and DSC analysis, and the results are summarized in Table 1. Two steps were observed in N₂ atmosphere thermal degradation of all samples, as shown in Figure 5a. The first step between 160 and 210 °C might result from the presence of labile methyl group present in polymer structure. This labile methyl group may belong to bisphenol A, or dianhydride, some residuals during the PEI synthesis process [2]. The second step is the main decomposition of the PEI matrix, due to the cleavage of phenyl-phthalimide bonds [2]. As shown in Figure 5a, the decomposition temperature was increased with increasing *c*-MWCNT–ODA concentration, and it reached the maximum value at 1.0 wt %, where it started to decrease with a further increase of the *c*-MWCNT–ODA concentration.

Table 1. Thermal properties of PEI and its composites.

Sample	Concentration (wt %)	Temp. at 10 wt % Weight Loss (°C)	Temp. at 30 wt % Weight Loss (°C)	Temp. at 40 wt % Weight Loss (°C)	<i>T_g</i> by DSC (°C)	<i>T_g</i> by DMA (°C)
<i>c</i> -MWCNT–ODA	0	488	519	563	216.9	218.2
	0.5	497	525	570	219.2	220.4
	1.0	506	536	597	224.4	225.6
	2.0	494	520	564	217.0	218.5
	5.0	498	528	583	221.8	222.3
<i>n</i> -MWCNT–ODA	0	488	519	563	216.9	218.2
	0.5	492	520	569	217.4	219.1
	1.0	498	529	592	221.6	223.9
	2.0	494	519	558	217.1	218.4
	5.0	496	523	574	219.1	220.5
MWCNT–COOH	0	488	519	563	216.9	218.2
	0.5	495	525	570	217.2	218.1
	1.0	491	536	597	217.4	219.0
	2.0	492	520	564	217.2	218.3
	5.0	485	522	549	217.8	219.5

As shown in Figure 5b and Table 1, it can be concluded, compared with neat PEI (*T_g* = 216.9 °C), that *T_g* is increased by about 8 °C after incorporating 1.0 wt % *c*-MWCNT–ODA, and 5 °C after incorporating 1.0 wt % *n*-MWCNT–ODA into PEI matrix. This also indicates the mobility of polymer chains is reduced due to the constraint effect of MWCNTs, and the interaction of MWCNT with PEI is obvious in the covalent functionalization more than non-covalent functionalization. As well as the effect on the thermal stability of ODA to PEI matrix, the over increasing content of ODA will decrease the *T_g* of nanocomposites. In addition, there is another smaller peak in DSC curves of 2.0 and 5.0 wt %, which may belong to the diffusion or melt of ODA chain. Since ODA prefers to react at the tube-ends or the defects on the sidewall of MWCNT, where the active areas are, this can induce the ODA chains to aggregate or form crystals on the surface of MWCNTs. The diffusion of the aggregated ODA chain or the melt of the crystallized ODA will lead to an obvious change of enthalpy. This peak is not

obvious when the content of ODA is low, or does not even exist in curves of 0.5 and 1.0 wt % functionalized MWCNTs.

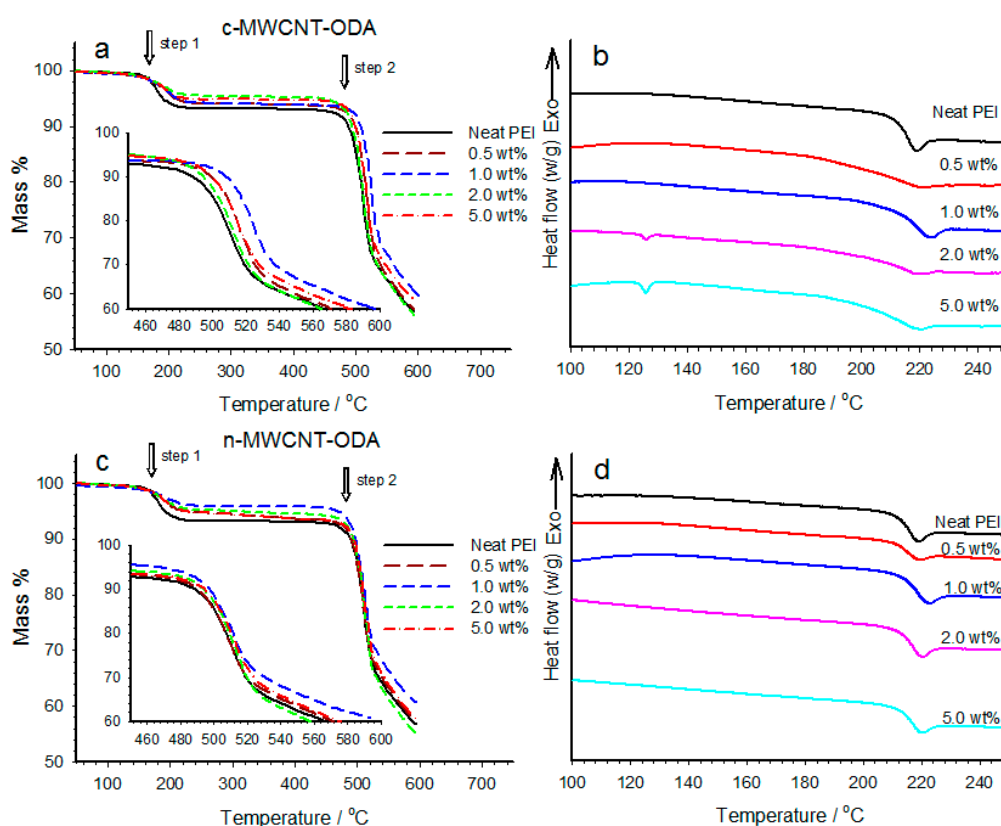


Figure 5. (a) The TGA weight loss curves and (b) DSC curves of PEI and composites with different MWCNT–ODA concentration, (c) The TGA weight loss curves and (d) DSC curves of PEI and composites with different *n*-MWCNT–ODA.

2.5. Mechanical Properties of the Composite Films

Figure 6a,b show the DMA curves as a function of temperature for PEI and its nanocomposites. As shown in Figure 6a, the storage modulus (E') for the PEI composites with the *c*-MWCNT–ODA are higher than that of pure PEI, and the storage modulus increased significantly with increasing *c*-MWCNT–ODA concentration from 0 to 1.0 wt %, and at the concentration of 2.0 wt %, it decreases, but with further increasing *c*-MWCNT–ODA, 5.0 wt % in Figure 6a, the modulus increases again. The results are summarized in Table 2. The storage modulus at 50 °C is 3.31 GPa for the composite containing 1.0 wt % *c*-MWCNT–ODA, which exhibits about 70% increment compared with neat PEI of 1.95 GPa. The significant improvement in the storage modulus of PEI nanocomposites is ascribed to the combined effect of high performance and fine dispersion of high aspect ratio MWCNT filler. This is coincident with the thermal properties of PEI composites. The existence of crystalline ODA has a negative effect on the modulus of the PEI matrix, and with the increasing of ODA proportion in matrix, the mechanical property of PEI composite will be weakened, which induces the storage modulus of composites with 2.0% *c*-MWCNT–ODA to be lower than that of PEI with 1.0 wt % MWCNT. The similar trend is observed in Figure 6b of PEI with *n*-MWCNT–ODA.

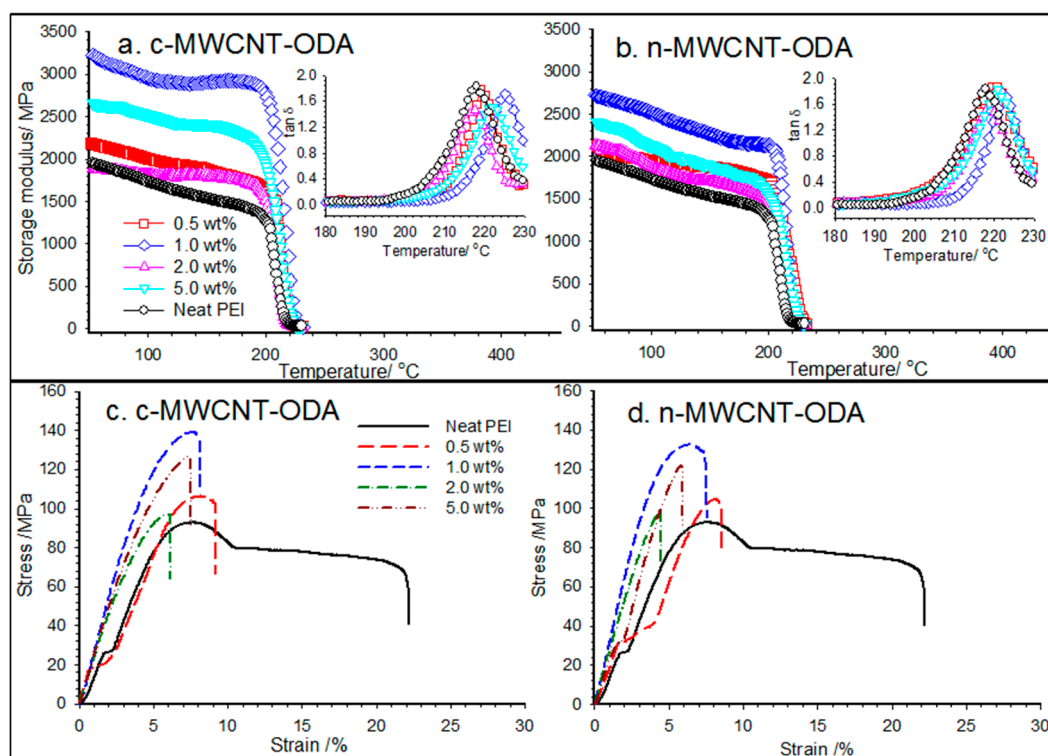


Figure 6. Mechanical properties for PEI and its composites with different modified MWCNT concentration: (a,b) DMA results, inset is the $\tan\delta$ versus temperature; and (c,d) typical stress-strain curves.

Table 2. Mechanical properties of neat PEI and its composites.

Sample	Concentration (wt %)	Storage Modulus at 50°C (GPa)	Storage Modulus at 200°C (GPa)	Tensile Strength (MPa)	Tensile Modulus (GPa)	Elongation at Break (%)
c-MWCNT-ODA	0	1.95	1.27	78.6	1.67	22
	0.5	2.19	1.63	103	2.15	9.2
	1.0	3.31	2.77	137	2.78	8.1
	2.0	1.92	1.51	96.9	2.07	6.2
	5.0	2.68	1.90	126	2.46	7.2
n-MWCNT-ODA	0	1.95	1.27	78.6	1.67	22
	0.5	2.12	1.60	101	2.02	8.5
	1.0	2.72	2.14	128	2.55	7.4
	2.0	2.13	1.46	99.7	1.96	4.7
	5.0	2.40	1.54	120	2.49	5.9
MWCNT-COOH	0	1.95	1.27	78.6	1.67	22
	0.5	2.17	1.59	-	-	-
	1.0	2.02	1.54	-	-	-
	2.0	1.90	1.48	-	-	-
ODA	0.5	-	-	80.5	1.64	10.7
	1.0	-	-	75.0	1.51	8.5
	5.0	-	-	66.4	1.40	6.5

From Table 2, we can also find that with the same MWCNT concentration, the storage modulus of PEI/*c*-MWCNT-ODA is much larger than that of PEI/*n*-MWCNT-ODA. This result indicates that the mechanical properties of PEI MWCNT composite with covalent modification are better than those of composites with non-covalent modification. Due to the homogenous dispersion of MWCNTs in PEI matrix, the high performance of the nanocomposites is obtained. Due to the strong interfacial interaction between MWCNTs and PEI, MWCNT can be wrapped by PEI, and the strong adhesion of MWCNT with PEI make PEI chains stiffer and more rigid. In the structure of *c*-MWCNT-ODA, the grafting of ODA to the MWCNTs backbone makes the *c*-MWCNT-ODA have many branches clinging outside, like the whiskers in brush. The existence of the whiskers makes the adhesion of *c*-MWCNT-ODA with PEI easier, and the PEI chain can be caught tightly by *c*-MWCNT-ODA. While the interaction of ODA and MWCNT in *n*-MWCNT-ODA is weaker than *c*-MWCNT-ODA, and the electrostatic force between ODA and MWCNT is weakened when ODA molecules interacts with PEI chain, the MWCNTs cannot adhere to PEI chain tightly. Herein, PEI chains with *c*-MWCNT-ODA modification are stiffer and stronger than with *n*-MWCNT-ODA modification, which lead to a higher storage modulus.

Typical stress-strain curves for neat PEI and its nanocomposites with different *c*-MWCNT-ODA concentration and *c*-MWCNT-ODA are shown in Figure 6c,d. All of the results are summarized in Table 2. For *c*-MWCNT-ODA as an example, as shown in Figure 6c, it can be seen that the tensile properties of the nanocomposites with 1.0 wt % *c*-MWCNT-ODA is the best, the trend of the tensile properties with increasing *c*-MWCNT-ODA is in agreement with DMA results. The tensile strength of PEI is improved by about 74% from 78.6 to 137 MPa; and the tensile modulus is improved by about 66% from 1.67 to 2.78 GPa. A pronounced yield and post-yield drop are observed for neat PEI while there is no noticeable yield for *c*-MWCNT-ODA-reinforced PEI nanocomposites. Similar results are observed in nanocomposites with *n*-MWCNT-ODA-reinforced, as shown in Figure 6d. Therefore, by adding a small amount of the functionalized MWCNT, the nanocomposite films become stronger due to the strong interfacial interactions between the nanotubes and the PEI matrix. The properties of nanocomposites are not always increasing by increasing the ODA-functionalized MWCNT concentration. One possible reason is the agglomeration of MWCNTs would partially occur with increasing MWCNT concentration. Another reason is the existence of ODA molecules.

To reveal the influence of ODA on the properties of nanocomposites, the tensile properties of PEI-only composites with loading different ODA concentrations are investigated. As shown in Table 2, the properties of composites are affected by increasing more ODA content. When the ODA content is low, less than 0.5 wt %, where tensile properties change a little, within the fluctuation range of 5%; while further increasing the loading of ODA, the tensile strength will decrease, and when it reaches 5.0 wt %, the tensile strength is reduced by 16%, and the tensile modulus is reduced by 11%. As for nanocomposites, when the loading of ODA-functionalized MWCNT is less than 1.0 wt % (the concentration of ODA in the matrix is less than 0.5 wt %), the influence of ODA on the properties is negligible, and the good dispersion of MWCNT in the PEI matrix displayed an effectiveness of the functionalized carbon nanotubes as a reinforcement agents, so the thermal properties and mechanical properties are enforced strongly with adding functionalized MWCNT; while when the loading of ODA-functionalized MWCNT is in excess of 1.0 wt %, for example 2.0 wt % MWCNT-ODA (the loading of ODA is calculated about 0.7 wt %), it will have a contrary result. As a result of the increase of network formation for MWCNTs,

the thermal and mechanical properties are improved again with further increasing *c*-MWCNT–ODA or *n*-MWCNT–ODA content.

2.6. Electrical Properties of the Composite Films

Carbon nanotubes are one of the best nanofillers to improve the conductivity of materials. The room temperature volume resistivity of PEI and PEI/MWCNT composites with various concentrations of *n*-MWCNT–ODA and *c*-MWCNT–ODA are shown in Figure 7. Almost identical resistivity curves are obtained. As discussed before, both covalent and non-covalent functionalization brought a little damage to MWCNT surface morphology, but this modification did not affect its intrinsic electrical property significantly. The conductivity of CNT-based polymer nanocomposite is mainly dependent to the concentration and dispersion of CNTs in matrix, the intrinsic structure of CNTs, and a good connection with each other. In our electrical conductivity test, the same concentration and similar dispersion of modified MWCNT in nanocomposites displayed an approximate change in volume resistivity of PEI composite with *c*-MWCNT–ODA and *n*-MWCNT–ODA. As shown in Figure 7, the electrical resistivity generally decreases with increasing the content of functionalized MWCNT. It decreases slightly when the MWCNT content was at 0.1 wt %, from 3.82×10^{16} to 2.06×10^{16} $\Omega\cdot\text{cm}$ for *c*-MWCNT–ODA/PEI composite, and to 2.17×10^{16} $\Omega\cdot\text{cm}$ for *n*-MWCNT–ODA/PEI composite, respectively. At the small amount of MWCNT loading, the MWCNT could disperse separately in PEI matrix, the channel for transforming electrons could not be formed in a large area, which induces the little change of conductivity, and at this point, the composite is still an insulator. The volume resistivity sharply decreased from 2.17×10^{16} $\Omega\cdot\text{cm}$ at 0.1 wt % loading of *c*-MWCNT–ODA to 3.9×10^6 $\Omega\cdot\text{cm}$ at 0.5 wt % loading of *c*-MWCNT–ODA. The volume resistivity decreases dramatically about 10 orders of magnitude of the 0.5 wt % MWCNTs. The resistivity further decreased with increasing the loading of *c*-MWCNT–ODA, and can fall down to 1.17×10^4 $\Omega\cdot\text{cm}$ at 5.0 wt % loading of *c*-MWCNT–ODA. The same trend was observed by adding *n*-MWCNT–ODA. According to percolation theory, there is a critical concentration or percolation threshold at which a conductive path is formed in the composite causing the material to convert from a capacitor to a conductor. Figure 7 indicates that the percolation threshold of the nanocomposites in our study is between 0.1–0.5 wt %. According to Ounaies's report [41], the similar calculation of the percolation threshold is used in our experiment, and the obtained value is about 0.3 wt %, which means at this loading concentration of MWCNT, a network forms which provides channels for the electrons transferring throughout the whole matrix. The volume resistivity decreases dramatically about 12 orders of magnitude of the 5.0 wt % MWCNTs, which means that the conductivity property of PEI can be improved observably by using these functionalized MWCNT, and the chemical functionalization is stronger than physical functionalization (The volume resistivity of 5.0 wt % *n*-MWCNT–ODA/PEI composite is 1.91×10^4 $\Omega\cdot\text{cm}$). To our best knowledge, the obtained resistivity is one of the lowest values for MWCNT/polyimide composite films with the same MWCNT loading. Recently, Tang *et al.* [42] reported a percolation threshold of surfactant-assisted polyimide/MWCNTs nanocomposites is in range 0.5–1.0 wt % MWCNTs (from 3.08×10^9 to 2.98×10^6 $\Omega\cdot\text{cm}$), and the resistivity can be reduced to 8.02×10^4 $\Omega\cdot\text{cm}$ with loading 3.0 wt % MWCNT. Kumar *et al.* [2] found that the conductivity of PEI could be improved by using MWCNT via a facile solution processing

method, and the volume resistivity could be decreased to $10^5 \Omega \cdot \text{cm}$ of loading 5.0 wt % MWCNT, which is much higher than the value obtained in this experiment.

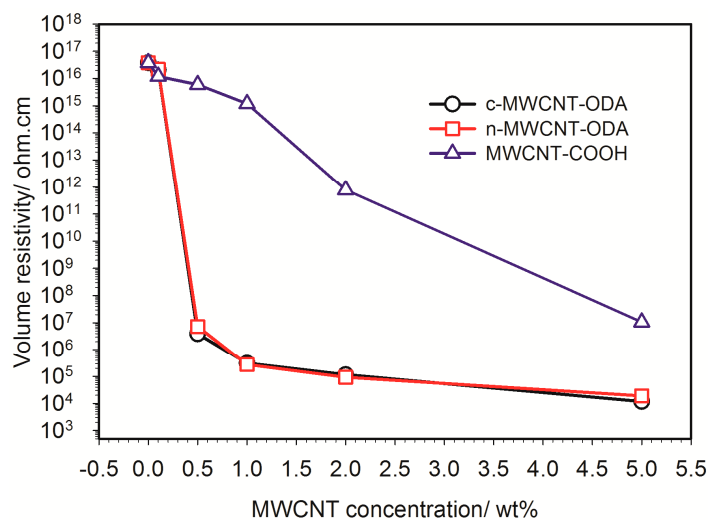


Figure 7. Volume resistivity of PEI and the composites with *c*-MWCNT–ODA, *n*-MWCNT–ODA and MWCNT–COOH at room temperature.

3. Experimental Section

3.1. Materials

Polyetherimide (PEI) in fine powder was supplied by SABIC Innovative Plastics (Riyadh, Saudi Arabia) under the trade name of Grade ULTEM 1000P. Carboxyl group functionalized MWCNTs (MWCNT–COOH, diameter is 10–20 nm, length is 5–30 μm and purity >95%) were purchased from GRAFEN INC. (KNT-MCH-CN2, Ankara, Turkey). Octadecylamine (ODA) was purchased from Sigma and used as received. The organic solvents, chloroform, oxalyl chloride, *N,N*-Dimethylformamide (DMF), tetrahydrofuran (THF), dichloromethane (DCM), and methanol were all purchased from Sigma-Aldrich (St Louis, MI, USA) and used without further purification.

3.2. Functionalization of MWCNT–COOH

3.2.1. Covalent Functionalization of ODA on MWCNT-COOH (*c*-MWCNT–ODA)

A sample of MWCNT with ODA covalent functionalization (*c*-MWCNT-ODA) was prepared as shown in Figure 8a. A mixture of 300 mg MWCNT, 40 mL oxalyl chloride and three drops of DMF was stirred at 70 °C for 24 h, and then it was centrifuged at 4000 rpm for 5 min followed by cooling. The extra oxalyl chloride was decanted and the remaining solid was washed with THF, and the supernatant was decanted after centrifugation. After repeating this step with THF four times, the remaining solid was dried at 60 °C in an oven overnight. The product, MWCNT–COCl, was obtained and further treated with mixing with ODA (6 g) at 100 °C for five days. After cooling, the solid was washed with a mixture of dichloromethane (DCM) and methanol (1:1). The supernatant was decanted after centrifugation. After repeating this step with the mixture solvent for four times, the *c*-MWCNT-ODA was obtained after drying the remaining solid at 60 °C in an oven for 24 h [36,37].

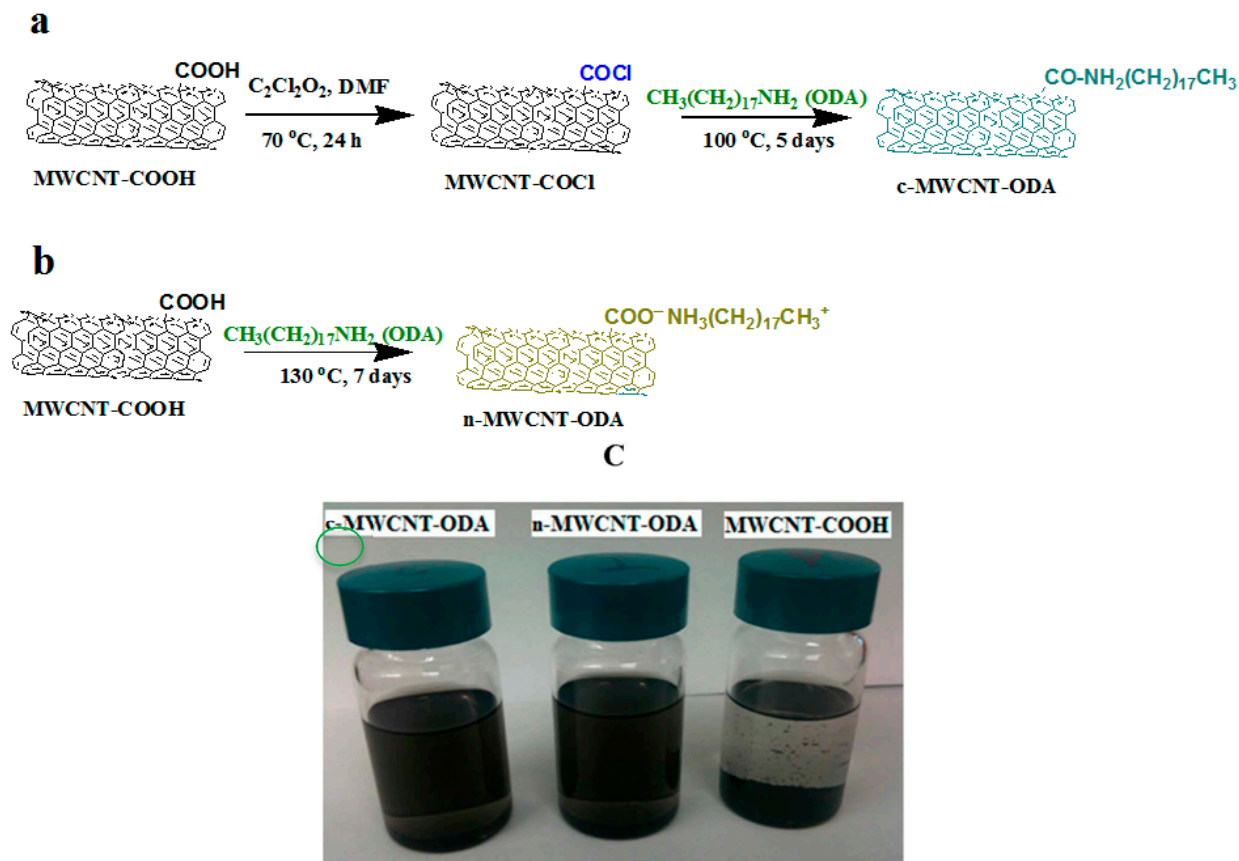


Figure 8. The preparation process of (a) *c*-MWCNT–ODA and (b) *n*-MWCNT–ODA; and (c) dispersion results of *c*-MWCNT–ODA, *n*-MWCNT–ODA, and pristine MWCNT–COOH (the samples were placed stably for one week after sonication for 30 min; the concentration was 0.2 wt %).

3.2.2. Non-Covalent Functionalization of ODA on MWCNT–COOH (*n*-MWCNT–ODA)

A sample of MWCNT with ODA non-covalent functionalization (*n*-MWCNT–ODA) was prepared as shown in Figure 8b. A mixture of 500 mg MWCNT and 6 g ODA was heated at 130 °C for seven days. After cooling to room temperature, the black solid was washed with dichloromethane (DCM) and methanol (1:1). After centrifugation, the supernatant was decanted. After repeating this step four times, the *n*-MWCNT–ODA was obtained by drying solid at 60 °C in an oven for 24 h [38].

3.3. Preparation of Composite Film

PEI (2 g) was completely dissolved into DCM (10 mL) and stirred for 2 h. The functionalized MWCNT of *c*-MWNT–ODA or *n*-MWCNT–ODA were dispersed separately into DCM under bath-type sonication for 1 h to form homogeneous suspension, and then it was mixed with the PEI solution. The mixture was stirred first for 1 h at room temperature, and then treated under bath-type sonication for 1 h. The obtained solutions were coated on a clean glass plate followed by solvent evaporation at room temperature for 24 h. The samples with about 0.3 mm thickness were dried at 80 °C for 24 h to remove any remaining solvent. A series of *c*-MWNT–ODA/PEI or *n*-MWNT–ODA/PEI nanocomposites

with functionalized MWCNT concentration of 0.1, 0.5, 1.0, 2.0, and 5.0 wt % in PEI solid contents were obtained following this procedure (Figure 9).

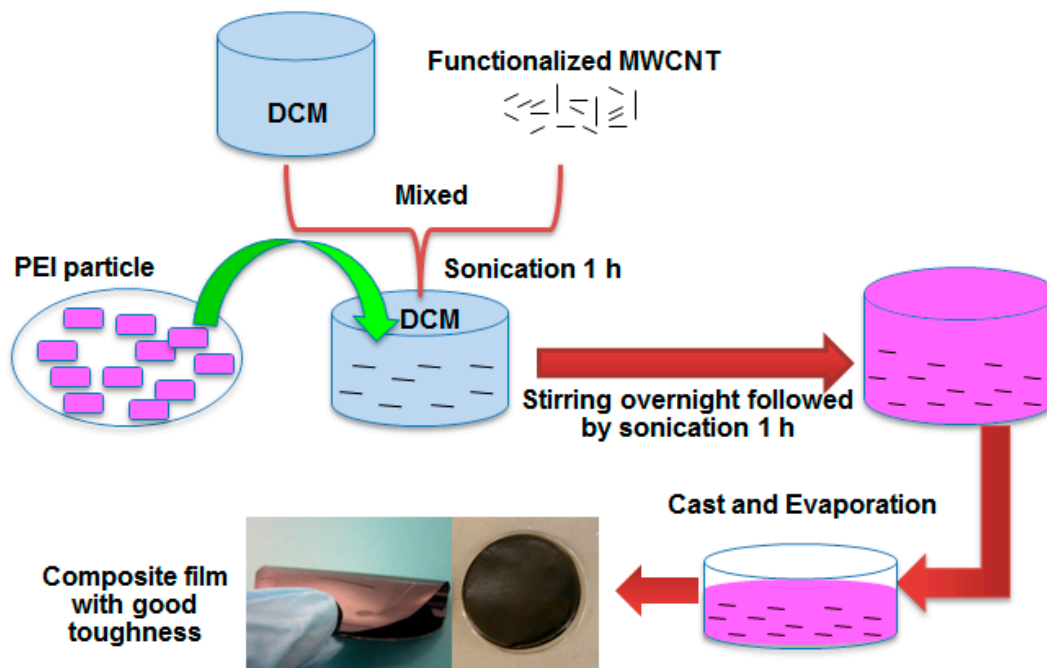


Figure 9. Process used for making PEI/MWCNT composite films.

3.4. Characterization

3.4.1. Characterization for the Functionalized MWCNT

Fourier transform infrared spectroscopy (FTIR) spectra of the *c*-MWCNT-ODA and *n*-MWCNT-ODA were recorded between 500 and 4000 cm^{-1} by a Thermo Nicolet iS10 (Madison, WI, USA). The X-ray powder diffraction (XRD) patterns were performed on the *c*-MWCNT-ODA and *n*-MWCNT-ODA samples by a Bruker D8 Advance (40 KV, 40 mA, Baden-Württemberg, Germany) with $\text{Cu K}\alpha$ ($\lambda = 1.5406 \text{ \AA}$) irradiation at a scanning rate of $2^\circ/\text{min}$ in the 2θ range of $10\text{--}40^\circ$. The decomposition behavior test was done through the thermogravimetric analysis (TGA) using Netzsch TG 209 F1 Iris at a temperature range of $30\text{--}600^\circ\text{C}$ under N_2 flow with a heating rate of $10^\circ\text{C}/\text{min}$.

3.4.2. Characterization of the Composite Films

Scanning electron microscope (SEM) (FEI, Quanta 600, Oregon, USA) was used to study the morphology of the fracture surface for the PEI and its composite film. The cryo-fractured surfaces were coated with a thin layer of gold (5 nm). The vacuum was on the order of $10^{-4}\text{--}10^{-6}$ mmHg during scanning of the composite samples. Transmission electron microscopy (TEM) analysis and energy-dispersive spectroscopy (EDS) were performed on a Tecnai T12 (FEI Company, Hillsboro, OR, USA) electron microscope at accelerated voltage of 120 kV. Dynamic mechanical thermal analysis (DMA) was performed on DMA 242C (Netzsch, Bavarian, Germany) in the thin tension mode, at a constant frequency of 1 Hz, with the static force at 0.3 N, the dynamic force at 0.2 N, a heating rate of 2 K/min under a nitrogen atmosphere and in the temperature range of 50 to 230°C . Tensile testing was

done on a commercial universal testing machine (Changchun Zhineng Company, Changchun, China) at room temperature with a crosshead speed of 5 mm/min. Specimens were cut from the casted films with 50 mm gauge lengths and 10 mm widths. The decomposition behavior of the composites was studied using thermogravimetric analysis (TGA) on a TG 209 F1 Iris (Netzsch) thermogravimetric analyzer in a nitrogen atmosphere from 30 to 600 °C, with a heating rate of 10 °C/min. The thermal behavior of the nanocomposites was studied using a differential scanning calorimeter (DSC 204 F1 Phoenix, Netzsch). The heating rate was 10 °C/min under a nitrogen atmosphere with a flow rate of 20 mL/min. The results of DMA, tensile strength and thermal properties were obtained by averaging three different specimens of each nanocomposite film.

The electrical conductivities of the samples were measured as follows: specimens were cut from the edge of each PEI nanocomposite film toward the center with 30 mm lengths, 10 mm widths, and about 0.3–0.5 mm thickness. A constant voltage of 100 V DC was applied across the specimen using a Keithley model 248 high voltage supply (USA). The current was monitored with a Keithley 6517B (Cleveland, OH, USA) electrometer. The results were obtained by averaging the conductivities from three different specimens of each nanocomposite film and each specimen was tested five times.

4. Conclusions

Well-dispersed multi-walled carbon nanotubes (MWCNT) in DCM were prepared by covalent and non-covalent functionalization with octadecylamine (ODA). Then the modified MWCNT suspensions were mixed with PEI solutions by stirring and sonication, and a simple MWCNT composite film was obtained by coating. The results showed a unique combination of properties, such as high electrical conductivity, high mechanical properties, and high thermal stability at low loading of MWCNTs, both covalent and non-covalent functionalization. SEM revealed the individual MWCNTs dispersed in the PEI matrix, which had a strong interfacial bonding with the PEI matrix. The presence of MWCNT increased the thermal stability and mechanical property by a significant amount at only 1.0 wt % MWCNT loading, which is the best value for the nanocomposites. Excess ODA gave a strong negative effect on the property of PEI matrix. Therefore, the thermal and mechanical properties will not improve further by only increasing modified-MWCNT content. The electrical conductivity was enforced by adding these two different MWCNTs, and the values increased dramatically by increasing MWCNT contents. It can be concluded that MWCNTs with covalent functionalization was better than that with non-covalent functionalization to improve the thermal and mechanical properties of PEI. The processing technique is easy and reproducible. It can be expanded to include other types of thermoplastics such as polycarbonate (PC), polyamide (PA), polyether sulfone (PES), polyaryletherketone (PAEK), and so on.

Acknowledgments

The authors gratefully acknowledge the support from King Abdullah University of Science and Technology (KAUST, Thuwal, Saudi Arabia) and Saudi Aramco Company (Dhahran, Saudi Arabia).

Author Contributions

Ye Chen, Jing Tao, Alaa Ezzeddine, Remi Mahfouz, Abdullah Al-Shahrani and Gasan Alabedi executed the experiments, interpreted the data, designed the Figures, and wrote the manuscript. Niveen Khashab supervised the project.

Conflicts of Interest

The authors declare no conflict of interest.

References

1. Liu, T.X.; Tong, Y.J.; Zhang, W.D. Preparation and characterization of carbon nanotube/polyetherimide nanocomposite films. *Compos. Sci. Technol.* **2007**, *67*, 406–412.
2. Kumar, S.; Li, B.; Caceres, S.; Maguire, R.G.; Zhong, W.H. Dramatic property enhancement in polyetherimide using low-cost commercially functionalized multi-walled carbon nanotubes via a facile solution processing method. *Nanotechnology* **2009**, *20*, doi:10.1088/0957-4484/20/46/465708.
3. Goh, P.S.; Ng, B.C.; Ismail, A.F.; Aziz, M.; Sanip, S.M. Surfactant dispersed multi-walled carbon nanotube/polyetherimide nanocomposite membrane. *Solid State Sci.* **2010**, *12*, 2155–2162.
4. Kumar, S.; Sun, L.L.; Caceres, S.; Li, B.; Wood, W.; Perugini, A.; Maguire, R.G.; Zhong, W.H. Dynamic synergy of graphitic nanoplatelets and multi-walled carbon nanotubes in polyetherimide nanocomposites. *Nanotechnology* **2010**, *21*, doi:10.1088/0957-4484/21/10/105702.
5. Carfagna, C.; Amendola, E.; Nicolais, L.; Acierno, D.; Francescangeli, O.; Yang, B.; Rustichelli, F. Blends of a polyetherimide and a liquid-crystalline polymer—Fiber orientation and mechanical-properties. *J. Appl. Polym. Sci.* **1991**, *43*, 839–844.
6. Nayak, G.C.; Rajasekar, R.; Das, C.K. Effect of SiC coated MWCNTs on the thermal and mechanical properties of PEI/LCP blend. *Compos. A Appl. Sci. Manuf.* **2010**, *41*, 1662–1667.
7. Kumar, S.; Rath, T.; Mahaling, R.N.; Reddy, C.S.; Das, C.K.; Pandey, K.N.; Srivastava, R.B.; Yadaw, S.B. Study on mechanical, morphological and electrical properties of carbon nanofiber/polyetherimide composites. *Mater. Sci. Eng. B* **2007**, *141*, 61–70.
8. Li, B.; Wood, W.; Baker, L.; Sui, G.; Leer, C.; Zhong, W.H. Effectual dispersion of carbon nanofibers in polyetherimide composites and their mechanical and tribological properties. *Polym. Eng. Sci.* **2010**, *50*, 1914–1922.
9. Iijima, S. Helical microtubules of graphitic carbon. *Nature* **1991**, *354*, 56–58.
10. Coleman, J.N.; Khan, U.; Gun'ko, Y.K. Mechanical reinforcement of polymers using carbon nanotubes. *Adv. Mater.* **2006**, *18*, 689–706.
11. Coleman, J.N.; Khan, U.; Blau, W.J.; Gun'ko, Y.K. Small but strong: A review of the mechanical properties of carbon nanotube-polymer composites. *Carbon* **2006**, *44*, 1624–1652.
12. Moniruzzaman, M.; Winey, K.I. Polymer nanocomposites containing carbon nanotubes. *Macromolecules* **2006**, *39*, 5194–5205.
13. Diez-Pascual, A.M.; Martinez, G.; Martinez, M.T.; Gomez, M.A. Novel nanocomposites reinforced with hydroxylated poly(ether ether ketone)-grafted carbon nanotubes. *J. Mater. Chem.* **2010**, *20*, 8247–8256.

14. Xia, H.S.; Song, M. Preparation and characterization of polyurethane-carbon nanotube composites. *Soft Matter* **2005**, *1*, 386–394.
15. Spitalsky, Z.; Tasis, D.; Papagelis, K.; Galiotis, C. Carbon nanotube-polymer composites: Chemistry, processing, mechanical and electrical properties. *Prog. Polym. Sci.* **2010**, *35*, 357–401.
16. Gruner, G. Carbon nanotube films for transparent and plastic electronics. *J. Mater. Chem.* **2006**, *16*, 3533–3539.
17. Ma, P.C.; Siddiqui, N.A.; Marom, G.; Kim, J.K. Dispersion and functionalization of carbon nanotubes for polymer-based nanocomposites: A review. *Compos. A Appl. Sci. Manuf.* **2010**, *41*, 1345–1367.
18. Chakraborty, A.K.; Coleman, K.S. Poly(ethylene) glycol/single-walled carbon nanotube composites. *J. Nanosci. Nanotechnol.* **2008**, *8*, 4013–4016.
19. Bellayer, S.; Gilman, J.W.; Eidelman, N.; Bourbigot, S.; Flambard, X.; Fox, D.M.; de Long, H.C.; Trulove, P.C. Preparation of homogeneously dispersed multiwalled carbon nanotube/polystyrene nanocomposites via melt extrusion using trialkyl imidazolium compatibilizer. *Adv. Funct. Mater.* **2005**, *15*, 910–916.
20. Price, B.K.; Tour, J.M. Functionalization of single-walled carbon nanotubes “on water”. *J. Am. Chem. Soc.* **2006**, *128*, 12899–12904.
21. Hu, H.; Zhao, B.; Hamon, M.A.; Kamaras, K.; Itkis, M.E.; Haddon, R.C. Sidewall functionalization of single-walled carbon nanotubes by addition of dichlorocarbene. *J. Am. Chem. Soc.* **2003**, *125*, 14893–14900.
22. Coleman, K.S.; Bailey, S.R.; Fogden, S.; Green, M.L.H. Functionalization of single-walled carbon nanotubes via the bingel reaction. *J. Am. Chem. Soc.* **2003**, *125*, 8722–8723.
23. Ge, J.J.; Zhang, D.; Li, Q.; Hou, H.Q.; Graham, M.J.; Dai, L.M.; Harris, F.W.; Cheng, S.Z.D. Multiwalled carbon nanotubes with chemically grafted polyetherimides. *J. Am. Chem. Soc.* **2005**, *127*, 9984–9985.
24. Blake, R.; Coleman, J.N.; Byrne, M.T.; McCarthy, J.E.; Perova, T.S.; Blau, W.J.; Fonseca, A.; Nagy, J.B.; Gun’ko, Y.K. Reinforcement of poly(vinyl chloride) and polystyrene using chlorinated polypropylene grafted carbon nanotubes. *J. Mater. Chem.* **2006**, *16*, 4206–4213.
25. Krstic, V.; Duesberg, G.S.; Muster, J.; Burghard, M.; Roth, S. Langmuir-blodgett films of matrix-diluted single-walled carbon nanotubes. *Chem. Mater.* **1998**, *10*, 2338–2340.
26. Star, A.; Stoddart, J.F.; Steurman, D.; Diehl, M.; Boukai, A.; Wong, E.W.; Yang, X.; Chung, S.W.; Choi, H.; Heath, J.R. Preparation and properties of polymer-wrapped single-walled carbon nanotubes. *Angew. Chem. Int. Ed. Engl.* **2001**, *40*, 1721–1725.
27. Coleman, J.; Dalton, A.; Curran, S.; Rubio, A.; Davey, A.; Drury, A.; McCarthy, B.; Lahr, B.; Ajayan, P.; Roth, S.; *et al.* Phase separation of carbon nanotubes and turbostratic graphite using a functional organic polymer (vol 12, pg 213, 2000). *Adv. Mater.* **2000**, *12*, 213–216.
28. Li, L.Y.; Li, C.Y.; Ni, C.Y. Polymer crystallization-driven, periodic patterning on carbon nanotubes. *J. Am. Chem. Soc.* **2006**, *128*, 1692–1699.
29. Suri, A.; Chakraborty, A.K.; Coleman, K.S. A facile, solvent-free, noncovalent, and nondisruptive route to functionalize single-wall carbon nanotubes using tertiary phosphines. *Chem. Mater.* **2008**, *20*, 1705–1709.

30. Zhang, L.; Tao, T.; Li, C.Z. Formation of polymer/carbon nanotubes nano-hybrid shish-kebab via non-isothermal crystallization. *Polymer* **2009**, *50*, 3835–3840.
31. Vaisman, L.; Wagner, H.D.; Marom, G. The role of surfactants in dispersion of carbon nanotubes. *Adv. Colloid Interface Sci.* **2006**, *128*, 37–46.
32. Amirilargani, M.; Tofighy, M.A.; Mohammadi, T.; Sadatnia, B. Novel poly(vinyl alcohol)/multiwalled carbon nanotube nanocomposite membranes for pervaporation dehydration of Isopropanol: Poly(sodium 4-styrenesulfonate) as a functionalization agent. *Ind. Eng. Chem. Res.* **2014**, *53*, 12819–12829.
33. Karousis, N.; Tagmatarchis, N.; Tasis, D. Current progress on the chemical modification of carbon nanotubes. *Chem. Rev.* **2010**, *110*, 5366–5397.
34. Siochi, E.J.; Working, D.C.; Park, C.; Lillehei, P.T.; Rouse, J.H.; Topping, C.C.; Bhattacharyya, A.R.; Kumar, S. Melt processing of SWCNT-polyimide nanocomposite fibers. *Compos. B Eng.* **2004**, *35*, 439–446.
35. Isayev, A.I.; Kumar, R.; Lewis, T.M. Ultrasound assisted twin screw extrusion of polymer-nanocomposites containing carbon nanotubes. *Polymer* **2009**, *50*, 250–260.
36. Chen, J.; Hamon, M.A.; Hu, H.; Chen, Y.S.; Rao, A.M.; Eklund, P.C.; Haddon, R.C. Solution properties of single-walled carbon nanotubes. *Science* **1998**, *282*, 95–98.
37. Hamon, M.A.; Chen, J.; Hu, H.; Chen, Y.S.; Itkis, M.E.; Rao, A.M.; Eklund, P.C.; Haddon, R.C. Dissolution of single-walled carbon nanotubes. *Adv. Mater.* **1999**, *11*, 834–840.
38. Chen, J.; Rao, A.M.; Lyuksyutov, S.; Itkis, M.E.; Hamon, M.A.; Hu, H.; Cohn, R.W.; Eklund, P.C.; Colbert, D.T.; Smalley, R.E.; *et al.* Dissolution of full-length single-walled carbon nanotubes. *J. Phys. Chem. B* **2001**, *105*, 2525–2528.
39. Xu, M.; Huang, Q.H.; Chen, Q.; Guo, P.S.; Sun, Z. Synthesis and characterization of octadecylamine grafted multi-walled carbon nanotubes. *Chem. Phys. Lett.* **2003**, *375*, 598–604.
40. Salavagione, H.J.; Martinez, G.; Marco, C. A polymer/solvent synergetic effect to improve the solubility of modified multiwalled carbon nanotubes. *J. Mater. Chem.* **2012**, *22*, 7020–7027.
41. Ounaies, Z.; Park, C.; Wise, K.E.; Siochi, E.J.; Harrison, J.S. Electrical properties of single wall carbon nanotube reinforced polyimide composites. *Compos. Sci. Technol.* **2003**, *63*, 1637–1646.
42. Tang, Q.Y.; Chan, Y.C.; Wong, N.B.; Cheung, R. Surfactant-assisted processing of polyimide/multiwall carbon nanotube nanocomposites for microelectronics applications. *Polym. Int.* **2010**, *59*, 1240–1245.